ISSN 1063-7737, Astronomy Letters, 2015, Vol. 41, No. 9, pp. 489–500. © Pleiades Publishing, Inc., 2015.
Original Russian Text © A.K. Dambis, L.N. Berdnikov, Yu.N. Efremov, A.Yu. Kniazev, A.S. Rastorguev, E.V. Glushkova, V.V. Kravtsov, D.G. Turner, D.J. Majaess, R. Sefako, 2015, published in Pis'ma v Astronomicheskiĭ Zhurnal, 2015, Vol. 41, No. 9, pp. 533–544.

Classical Cepheids and the Spiral Structure of the Milky Way

A. K. Dambis[1*], L. N. Berdnikov[1,2], Yu. N. Efremov[1], A. Yu. Kniazev[1,3,4], A. S. Rastorguev[1], E. V. Glushkova[1], V. V. Kravtsov[1,5], D. G. Turner[6], D. J. Majaess[6], and R. Sefako[3]

[1]*Sternberg Astronomical Institute, Moscow State University, Universitetskii pr. 13, Moscow, 119992 Russia*

[2]*Astronomy and Astrophysics Research Division, Entoto Observatory and Research Center, P.O.Box 8412, Addis Ababa, Ethiopia*

[3]*South African Astronomical Observatory, P.O. Box 9, Observatory, Cape Town, 7935, South Africa*

[4]*Southern African Large Telescope, P.O. Box 9, Observatory, Cape Town, 7935, South Africa*

[5]*Department of Physics, Faculty of Natural Sciences, University of Atacama, Copayapu 485, Copiapó, Chile*

[6]*Department of Astronomy and Physics, Saint Mary's University, Halifax, NS B3H 3C3, Canada*

Received April 1, 2015

Abstract—We use data on space distribution of the currently most complete sample of Cepheids with reliable distances (565 stars), located within ∼5 kpc from the Sun, to study the spiral pattern of the Milky Way galaxy. We estimate the pitch angle as 9°−10°; the most accurate estimate, $i = 9.5° \pm 0.1°$, was obtained assuming the existence of a global four-armed spiral pattern; the solar phase angle in the spiral pattern is $\chi_\odot = -121° \pm 3°$. Comparing positions of the spiral arms delineated by classical Cepheids and galactic masers, with the age difference of these objects in mind, we estimate the rotation angular speed of the spiral pattern to be $\Omega_P = 25.2 \pm 0.5$ km s^{-1}kpc^{-1}.

DOI: 10.1134/S1063773715090017

Keywords: *Galactic structure, Cepheids, spiral arms.*

INTRODUCTION

Positions of spiral arms in our Galaxy are still a topic of debate. Thus, the distribution of neutral hydrogen clearly reveals two spiral arms, the Carina–Sagittarius arm and the Cygnus arm (Nakanishi and Sofue, 2003; Levine et al. 2006). Englmaier and Gerhard (1999), Englmaier et al. (2011), Hou et al. (2009) pointed out that the four-armed spiral pattern fitted well the distribution of neutral (H I), molecular (H_2), and ionized (H II) hydrogen. At the same time, Pohl et al. (2008) suggested a two-armed model based on their simulation of gas streaming motions. Russell (2003), it turn, derived a four-armed spiral pattern based on the distribution of star-forming regions; Efremov (2011) also pointed out that data on molecular and neutral hydrogen regions were in agreement with the four-armed spiral pattern as well, whose fragments were the most pronounced Carina and Cygnus arms, with regular intervals between superclouds of atomic and molecular hydrogen. A more detailed picture can be gained from studies of the distribution of stars that concentrate to the spiral arms.

According to observations, gas and young stars in other spiral galaxies concentrate practically to the same spiral arms and hence young stars and star clusters should trace the spiral pattern well enough. The problem is that we reside inside the Milky Way's thin disk and cannot look at it as at external galaxies. Consequently, spiral structure tracers should be objects with reliably determined distances, observable at large distances. Very promising from this point of view are galactic masers that are recently widely used for studies of the Galaxy's structure and kinematics. This is due to VLBI observations of masers being able not only to provide their very accurate parallaxes and proper motions but also to give reasonably accurate estimates of their radial velocities (Kim et al. 2008; Reid et al. 2009; Rygl et al. 2010; Bobylev and Bajkova 2013). However, the number of masers with precisely measured parameters (about 130 objects) is still insufficient for a detailed study of the Galaxy's spiral pattern. At the same time, classical Cepheids, also comparatively young stars whose distances can be determined very accurately from the period–luminosity relation, appear to be among the objects best suited for the task. Thus, a recent study of the Andromeda galaxy (M31) re-

*E-mail: mirage@sai.msu.ru

sulted in the discovery of more than 2000 Cepheids (Kodric et al. 2013); virtually all of them (with the exception of 150 Cepheids of the halo population) are concentrated to spiral arms. We have every reason to expect a similar concentration from Cepheids of our own Galaxy.

Thanks to extended multicolor photometry collected during our many-year observations of Galactic Cepheids (Berdnikov 2008; Berdnikov et al. 2011, 2014) and to the reliably established Cepheid period-luminosity relation (Berdnikov et al. 2000), we have everything needed to use these stars as spiral-arm tracers out to a heliocentric distance of about 5 kpc and hence for a reliable determination of the spiral pattern's parameters, in the assumption that it is regular.

OBSERVATIONAL DATA FOR MILKY WAY CEPHEIDS

Virtually for all Galactic Cepheids contained in the General Catalogue of Variable Stars (Samus et al. 2007–2012), Berdnikov et al. (2000) and Berdnikov (2006) published photometric parameters based on extensive photometry obtained with 0.5 to 1 m reflectors of the Maidanak Observatory (Republic of Uzbekistan), Cerro Tololo and Las Campanas observatories (Chile), and South African Astronomical Observatory. CCD monitoring of the southern sky performed as a part of the ASAS project (Pojmanski 2002) resulted in the discovery of numerous new variable stars, about a thousand of them classified as Cepheids by the authors of the ASAS project. However, ASAS project used cameras with short focal lengths, and Cepheid data solely from these telescopes do not permit a reliable distance determination. For this reason, we performed numerous CCD observations of 164 classical Cepheids from the ASAS-3 catalog during nine observing runs between April 2005 and January 2013 with the 76-cm telescope of the South African Astronomical Observatory (Republic of South Africa) and the 40-cm telescope of the Cerro Armazones Observatory of the Catholic University (Chile) (Berdnikov et al. 2009a, 2009b, 2011, 2015). The observations were obtained with an SBIG SBIG ST-10XME CCD camera and a single-channel pulse-counting photometer equipped with the BVI_C filters of the Kron–Cousins system (Cousins 1976). In our study of the distribution of classical Cepheids in the Galaxy, we use the updated version of the catalog of Cepheid light-curve parameters (Berdnikov et al. 2000) that contains 674 stars. The procedure of deriving distances is based on the period-luminosity relation in the K infrared band (Berdnikov et al. 1996), combined with the period–normal color $(B-V)$ relation from Dean et al. (1978). Since the underlying distance-scale calibration yields $R_0 = 7.1$ kpc for the distance estimate between the Sun and the Galaxy's center, the same estimate being used when taking into account the influence of the radial chemical-abundance gradient on color indices, we adopt it in this paper for consistency with the derived Cepheid distances. Note however that our results, expressed in terms of θ and R_G/R_0, remain virtually unchanged even if we determine distances using the more recent period–luminosity relation by Fouque et al. (2007) and, at the same time, upscale R_0 to ∼8.0 kpc.

SPIRAL ARMS

Figure 1 shows the distribution of our Cepheid sample projected onto the Galaxy's plane. The distribution of the same Cepheids in the $\ln(R_G/R_0)$—Galactocentric azimuth (θ) coordinates is presented in Fig. 2. The latter diagram is more convenient for identifying eventual spiral patterns because logarithmic spirals,

$$R_G/R_0 = a_0 e^{(\theta-\theta_0)\tan i} \qquad (1)$$

become straight lines in these coordinates:

$$\ln(R_G/R_0) = \alpha_0 + (\theta-\theta_0)\tan i, \qquad (2)$$

where $\alpha_0 = \ln a_0$, i is the pitch angle of the spiral, and θ_0 is an arbitrary initial angle, here set to zero, $\theta_0 = 0$ (cf. Bobylev and Bajkova 2013). It appears from the figure that the sample becomes very incomplete outside the $-0.7 \le \theta \le +0.3$, $-0.45 \le \ln(R_G/R_0) \le +0.7$ region, outlined with a dashed annular sector and a dashed rectangle, respectively in Figs. 1 and 2. Hereafter we use only the 565 stars located within this sector/rectangle in our search for fragments of the spiral pattern.

Search for the Major Spiral Arm Fragment

Given that the equation of a logarithmic spiral in the $\theta - \ln(R_G/R_0)$ coordinates is linear, the search for fragments of the spiral pattern in the distribution of Cepheids is reduced to identification, in Fig. 2, of linear chains that have minimal thickness (i.e., minimal cross-chain scatter) and, simultaneously, the largest possible number of stars. To this end, we use a slightly modified version of the "simple approach" described by Guerra and Pascucci (2001). The idea of this approach is "to search for the optimal line among those defined by pairs of points in the dataset". In the original version of the approach described in the paper cited above, a certain limiting "distance" from the two-point line, ϵ, is fixed, and the best line is considered to be that with the largest number of sample points, n, within this distance. Our approach

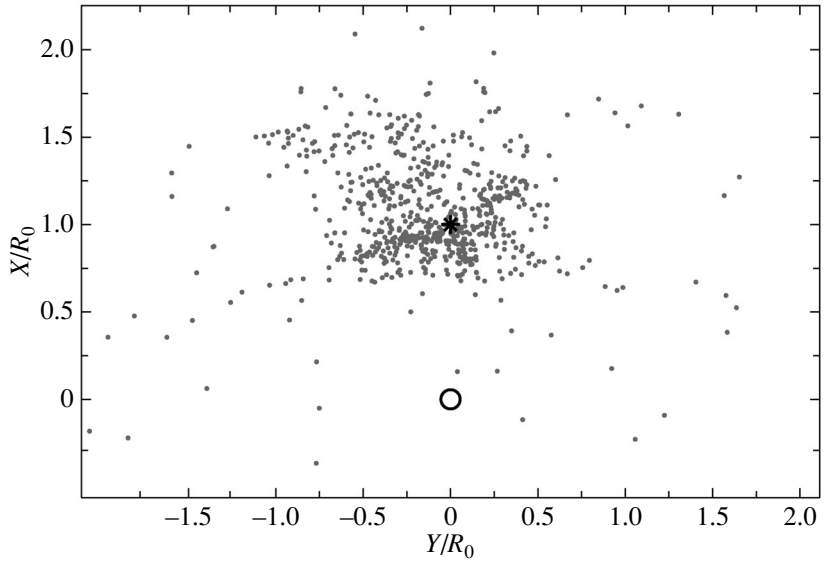

Fig. 1. Distribution of classical Cepheids projected onto the Galactic plane. The big circle and asterisk are respectively positions of the Galaxy's center and the Sun.

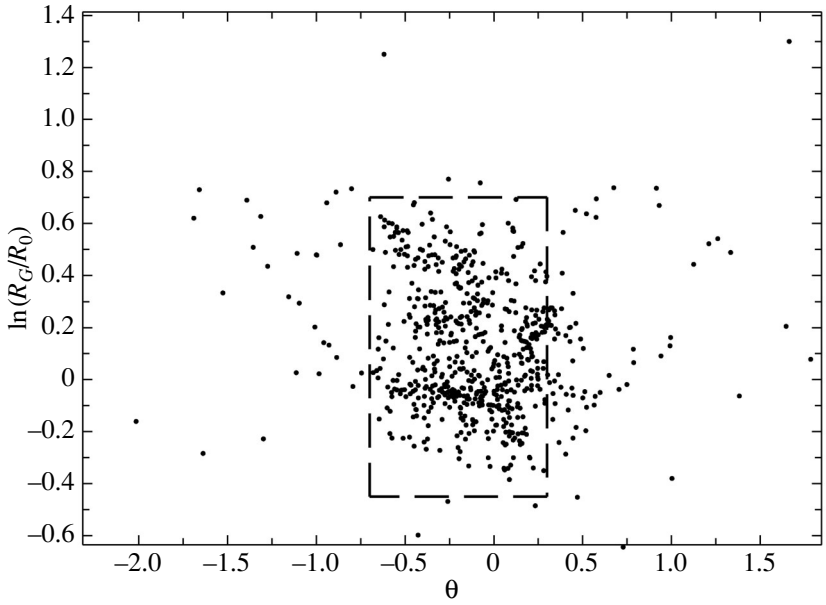

Fig. 2. Distribution of classical Cepheids in the $\ln(R_G/R_0)$ – Galactocentric azimuth θ coordinates. The dashed rectangle is the "relative completeness" region of the sample.

differs in that, instead, we fix the number n of stars closest to a straight line and look for a straight-line segment with the minimal rms scatter of objects around it. More specifically, for each two-point line in the sample, we find n points closest to it (including the two line-defining points) and determine the mean squared deviation of the selected n points from the straight line along the $\ln(R_G/R_0)$ coordinate. Our best n-point line is that with the smallest squared deviation of the n points closest to it. To identify the dominating spiral in the distribution of Cepheids, we search for lines, best in the discussed sense, on the

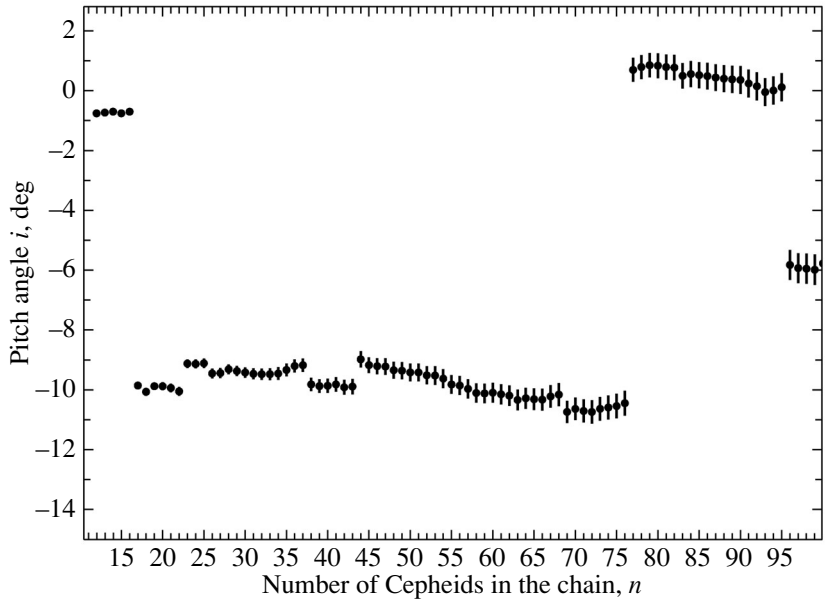

Fig. 3. Pitch angle i of the minimal-scatter chain versus the number of stars n.

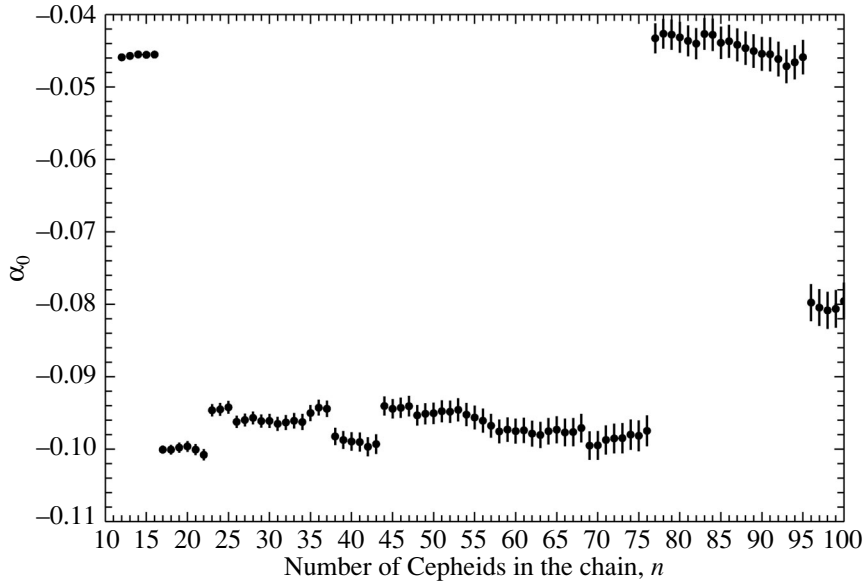

Fig. 4. Parameter α_0 of the chain with the minimal transversal scatter versus the number of stars n.

$\theta - \ln(R_G/R_0)$ plane, for n values in the $n = 10-100$ range and plot the relations of these straight lines' parameters (α_0 and $\tan i$) on n. The resulting relations, $\alpha_0(n)$ and $i(n)$, are displayed for our sample of 565 Cepheids in Figs. 3 and 4. It appears from the figures that both parameters remain practically unchanged in the $n = 17-76$ range (with $\alpha_0(n)$ between -0.094 and -0.102, $i(n)$ between 8.98° and 10.74°), changing abruptly with the further increase of n. Therefore we have all reasons to assume that the chain of $n_{\max} = 76$ stars with the minimal scatter along the $\ln(R_G/R_0)$ coordinate outlines the major spiral in the considered distribution of Cepheids. The parameters of the dominant spiral (determined via the least-squares solution for the selected $n_{\max} =$

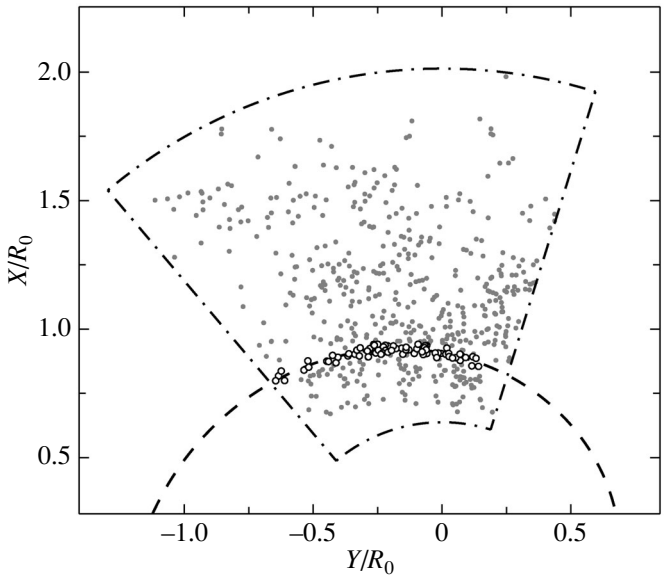

Fig. 5. The longest minimal-transversal-scatter chain of Cepheids, projected onto the Galactic plane. Circles are Cepheids of the longest chain ($n = 76$); the dashed curve is the corresponding logarithmic-spiral fit.

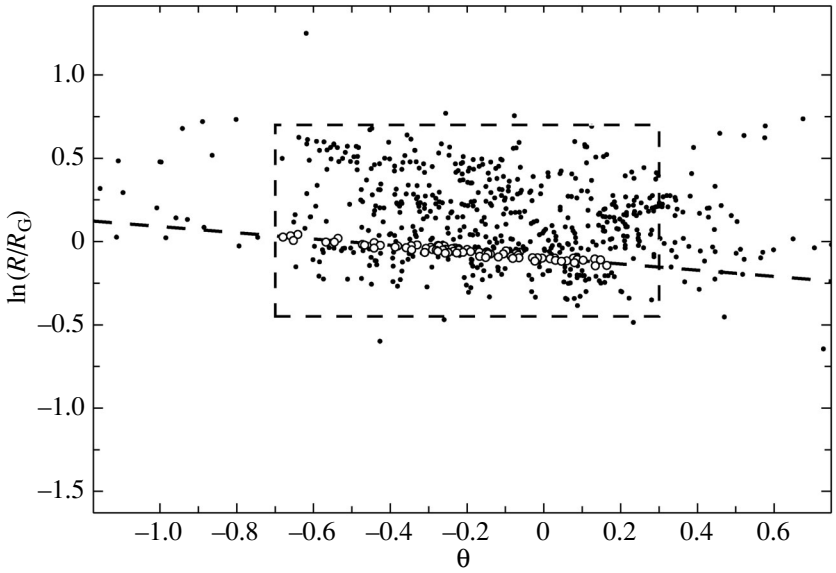

Fig. 6. The longest minimal-transversal-scatter chain of Cepheids in the $\theta-\ln(R_G/R_0)$ coordinates. Circles are Cepheids of the longest chain ($n = 76$), and the dashed line is the corresponding logarithmic-spiral fit.

76 stars) are:

$$\alpha_0 = -0.097 \pm 0.002 \quad \text{and} \qquad (3)$$
$$\tan i = -0.184 \pm 0.007 \quad (i = -10.45^\circ \pm 0.41^\circ)$$

with the rms deviation $\sigma(\ln(R_G/R_0)) = 0.013$.

Figures 5–7 show the thus identified chain of 76 Cepheids (open circles) with minimal scatter, respectively in the ordinary Cartesian XY coordinates and in the coordinates θ—$\ln(R_G/R_0)$. We see that the spiral traced by Eq. (3) coincides with what is usually referred to as the Carina–Sagittarius arm.

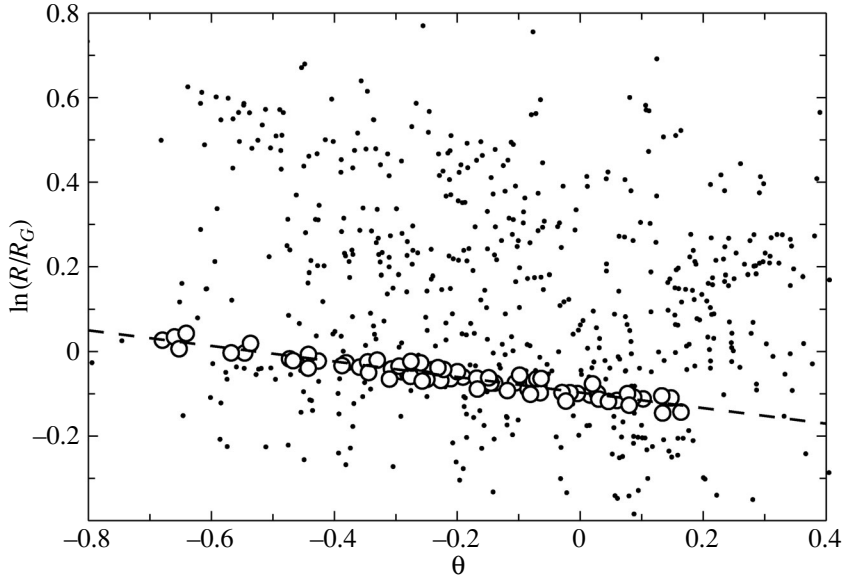

Fig. 7. Zoomed-in view of Fig. 6.

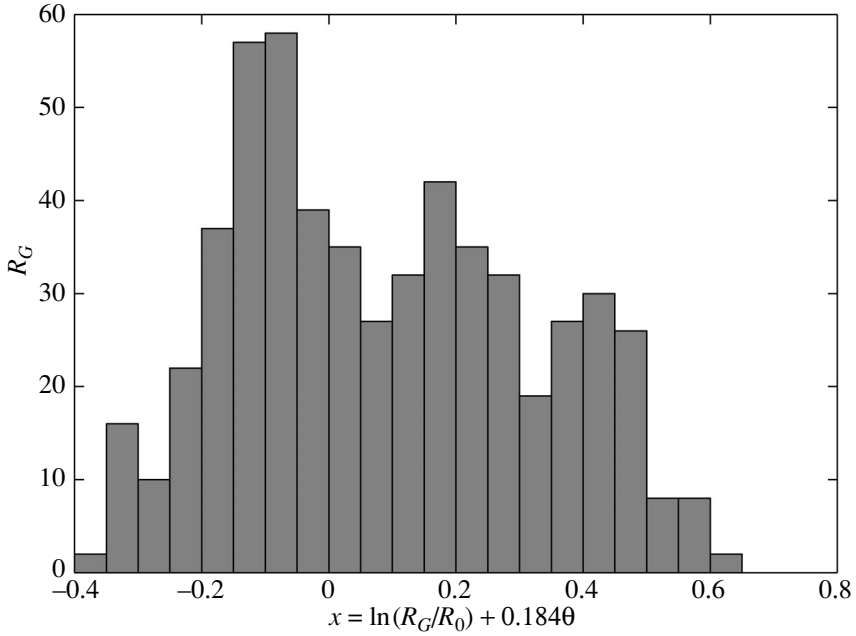

Fig. 8. Histogram of $x = \ln(R_G/R_0) + 0.184\theta$. The dips at $x = -0.275$, $+0.075$, and $+0.325$ separate the peaks at $x \sim -0.325$, -0.100, $+0.175$, and $+0.425$ that correspond to spiral arms.

Search for Other Spiral Fragments

We assume in the following that the pitch angles of other spiral-structure fragments in the space distribution of our Cepheid sample do not differ strongly from that of the main arm identified in the previous subsection. To identify additional spiral fragments, we plot the histogram of the parameter $x = \ln(R_G/R_0) + \tan i_{(\mathrm{Car-Sgr})}\theta$ (Fig. 8). The histogram clearly reveals three dips, at $x = -0.275$, $+0.075$, and $+0.325$, separating four peaks, at $x \sim -0.325$, -0.100, $+0.175$, and $+0.425$. The most conspicuous among them is the peak at $x \sim -0.100$ that corresponds to the already identified Carina–Sagittarius arm. Our next target is the spiral fragment that lies

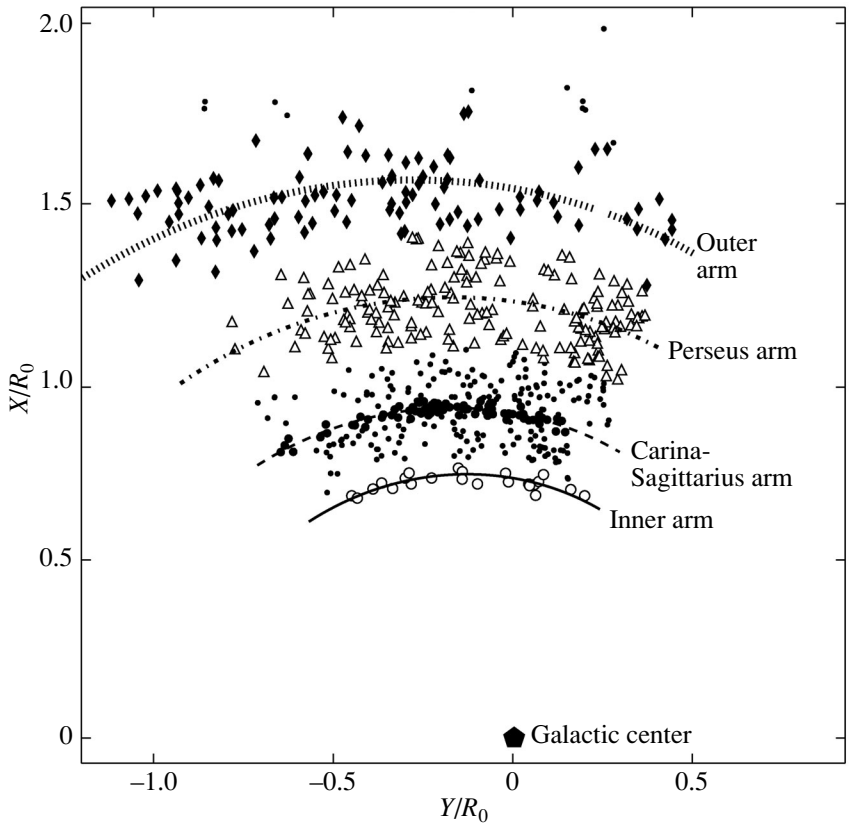

Fig. 9. Positions of spiral arms projected onto the Galactic plane. The stars that outline different arms are plotted as open circles (Inner arm), filled circles (Carina–Sagittarius arm), triangles (Perseus arm), and diamonds (Outer arm).

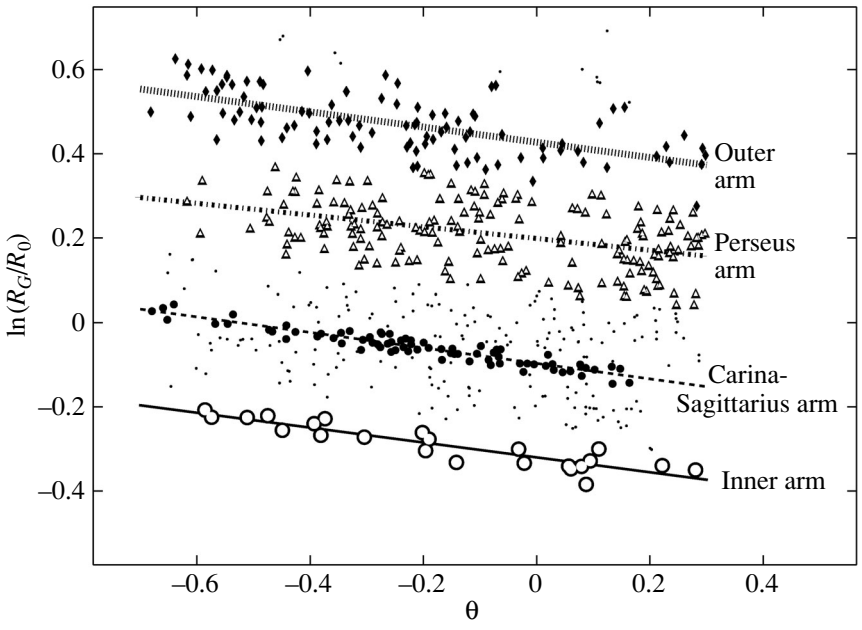

Fig. 10. Positions of spiral arms in the $\ln(R_G/R_0)$—θ coordinates. The symbols are the same as in Fig. 9.

Table 1. Parameters of spiral arms identified in the distribution of Cepheids

Arm	α_0	$\tan i$	i, deg	σ x	a_0, kpc	N
Inner	−0.320	−0.177	−10.02	0.021	5.16	23
	±0.005	±0.017	±0.95		±0.03	
Carina−Sagittarius	−0.097	−0.184	−10.45	0.013	6.44	76
	±0.002	±0.007	±0.41		±0.02	
Perseus	+0.199	−0.139	−7.91	0.067	8.66	168
	±0.005	±0.022	±1.24		±0.05	
Outer	+0.428	−0.181	−10.26	0.055	10.89	99
	±0.008	±0.022	±1.22		±0.09	
Mean		−0.180	−10.20			
		0.006	0.34			

behind the Carina−Sagittarius arm. in the direction to the Galactic center. To determine parameters of the spiral, we solve Eq. (2) for 23 stars with $x < -0.275$ by least squares:

$$\alpha_0 = -0.320 \pm 0.005 \quad \text{and} \quad \tan i = -0.177 \pm 0.017 \quad (i = -10.02^\circ \pm 0.95^\circ). \tag{4}$$

The rms scatter of the $\ln(R_G/R_0)$ coordinate for this arm is $\sigma(\ln(R_G/R_0)) = 0.021$.

The parameters of the remaining two arms are

$$\alpha_0 = +0.199 \pm 0.005 \quad \text{and} \quad \tan i = -0.139 \pm 0.022 \quad (i = -7.91^\circ \pm 1.24^\circ) \tag{5}$$

with the rms scatter $\sigma(\ln(R_G/R_0)) = 0.067$ (the Perseus arm), and

$$\alpha_0 = +0.428 \pm 0.008 \quad \text{and} \quad \tan i = -0.181 \pm 0.022 \quad (i = -10.26^\circ \pm 1.22^\circ) \tag{6}$$

with the rms scatter $\sigma(\ln(R_G/R_0)) = 0.055$ (the so-called Outer arm). We plot all the four arms and the corresponding Cepheids in Figs. 9 and 10.

We summarize the parameters of the identified arms in Table 1. Note that while the two arms closest to the Galactic center are narrow and well defined, the two external arms appear rather loose, "flocculent"; this might be due to the fact that the outer arms are beyond the corotation radius, while the inner arms are inside it. The pitch angles of all the arms agree rather well, except for the Perseus arm whose pitch angle is smaller than the mean by about 2σ. Table 2 presents the results of forcing the same pitch angle for all the four arms with weights proportional to $1/(\sigma x^2)$.

Table 2. Parameters of spiral arms derived in the assumption of the same pitch angle

Arm	α_0	a_0, kpc
Inner	−0.320	5.16
	±0.005	±0.03
Carina−Sagittarius	−0.096	6.45
	±0.002	±0.02
Perseus	+0.196	8.64
	±0.005	±0.05
Outer	+0.443	11.06
	±0.006	±0.06
$\tan i$	−0.177	
	±0.007	
i, deg	−10.03	
	±0.37	

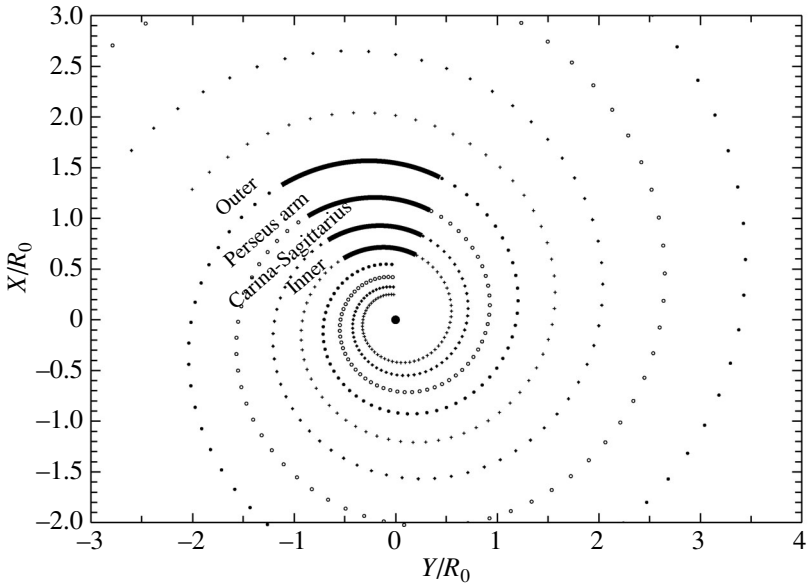

Fig. 11. The grand-design spiral pattern with the parameters from Table 3. The solid curves represent arm segments within the studied region ($-0.7 \le \theta \le +0.3$ and $-0.45 \le \ln(R_G/R_0) \le +0.7$).

Finally, we can assume that the observed spiral fragments represent a global grand-design four-armed pattern, i.e., that we observe fragments of four identical spirals, rotated with respect to each other by 90° in the position angle. In this case, we get a solution (the α_0 and a_0 parameters) presented in Table 3. We show the resulting grand-design spiral pattern in Fig. 11. Note that the pitch angle in this case ($i = -9.46° \pm 0.11°$) is, on the whole, consistent with the estimates obtained for individual spiral fragments ($i = -7.9°{-}10.5°$; cf. Table 1). However, if we try to fit the identified spiral fragments to the same global two- or three-armed pattern, we will obtain a pitch angle smaller in asbsolute value than the individual pitch angles of each of the four fragments ($|i| = 4.59° \pm 0.19°$ for the two-armed pattern and $|i| = 6.68° \pm 0.15°$ for the three-armed pattern), and the scatter of Cepheids with respect to the corresponding spirals (σx) will increase by factors of $\sim$2 and $\sim$2.3, respectively for the two-armed and three-armed pattern. Moreover, the pitch angle determined under the assumption of the three-armed structure is at the lowest limit of the distribution of observed pitch angles for the nearest spiral galaxies ($|i|_{\min} \sim 6.5°$, cf. Kennicutt and Hodge, 1982; Kendall et al.2015), and the "two-armed" pitch angle falls outside the observed distribution. Besides, three-armed spiral structures are very rare. These circumstances, taken together with our results, can be viewed as indirect evidence for the assumption of the four-armed spiral structure for our Galaxy. Based on the results presented in Table 3, we estimate the solar phase angle with respect to the crest of the spiral structure: $\chi_\odot = 360^* \alpha_{\text{Car–Sgr}}/(\alpha_{\text{Per}} - \alpha_{\text{Car–Sgr}}) = -121° \pm 3°$. Our

Table 3. Parameters of spiral arms determined assuming that they form a grand-design four-armed pattern

Arm	α_0	a_0, kpc
Inner	−0.349	5.01
	±0.002	±0.01
Carina−Sagittarius	−0.088	6.50
	±0.002	±0.01
Perseus	+0.174	8.45
	±0.002	±0.02
Outer	+0.436	10.98
	±0.006	±0.02
$\tan i$	−0.167	
	±0.002	
i, deg	−9.46	
	±0.11	

arm pitch-angle estimates agree reasonably well with the recent results by Bobylev and Bajkova (2014a), based on the distribution of Galactic masers (from 9.3° to 14.8°). Our mean estimates being somewhat smaller (from 9.46° to 10.20°) compared to the mean estimates from Bobylev and Bajkova (2014a) (from 9.9° to 13.7°) and the estimates of the global pitch angle obtained by Valle (2015) (from 12° to 14°), can be explained by larger ages of Cepheids (about 66 million years on the average) compared to the very young masers: as time passes, stars born in the arm "stretch" along the Galactic azimuth because the angular velocity of the Galactic rotation decreases with the distance from the center, i.e., because of the disk's differential rotation. The difference of our solar-phase estimate with respect to the spiral structure ($\chi_\odot = -121° \pm 3°$) from that of Bobylev and Bajkova (2014a) ($\chi_\odot = -140° \pm 3°$) can be explained by the shift of Cepheid-delineated arms in the solar neighborhood relative to the spiral-wave crests (which can be assumed to be practically coincident with maser-delineated arms) because of faster Galactic rotation (the angular speed of the Galactic rotation in the solar neighborhood, $\Omega(R_0) = 29.97$ km s^{-1}kpc^{-1}, is much higher than the speed of the spiral pattern, $\Omega_P = \sim$25 km s^{-1}kpc^{-1}; see the next Section).

ANGULAR SPEED OF THE SPIRAL PATTERN

To estimate the angular speed Ω_P of the Galactic spiral pattern, we compare positions of Cepheids in the identified spiral arms to positions of the corresponding arms (cf. Table 2 in Bobylev and Bajkova 2014a) traced by very young objects: Galactic masers with distances computed from high-accuracy parallaxes determined from VLBI observations:

$$\ln(R_0/R_G) = \alpha_{\rm maser} + \tan(i_{\rm maser})\theta. \qquad (7)$$

We begin with the best-defined Carina–Sagittarius arm. Its parameters determined from Galactic masers are $\alpha_{\rm maser} = -0.166$ and $\tan i_{\rm maser} = -0.163$. Given the very young age of maser sources, we assume that Eq. (7) defines the current location of the zero-age spiral arm (i.e. the locus where stars are currently born). We can rewrite Eq. (7) in the following reversed form:

$$\theta = (\ln(R_0/R_G) - \alpha_{\rm maser})/\tan(i_{\rm maser}). \qquad (8)$$

We then account for the shift (azimuthal turn) of the spiral wave during time t equal to the age of a particular Cepheid; at the time of its birth, the galactocentric azimuthal angle of the Cepheid θ can be written as:

$$\theta = [(\ln(R_0/R_G) - \alpha_{\rm maser})/\tan(i_{\rm maser})] - \Omega_P t. \qquad (9)$$

Finally, during time t, the Galaxy's differential rotation should move the Cepheid by the angle θ equal to $\Omega(R_G)t$, and hence the coordinate θ of the Cepheid should be:

$$\theta = [(\ln(R_0/R_G) - \alpha_{\rm maser})/\tan(i_{\rm maser})] \qquad (10)$$
$$- \Omega_P t + \Omega(R_G)t.$$

Consequently,

$$\Omega_P t = -\theta \qquad (11)$$
$$+ [(\ln(R_0/R_G) - \alpha_{\rm maser})/(\tan(i_{\rm maser}))] + \Omega(R_G)t.$$

We now determine the ages t for 76 Cepheids of the Carina–Sagittarius arm from their pulsation periods using the theoretical period–age relations computed by Bono et al. (2005) for Cepheids with solar metal abundances ($Z = 0.02$), pulsating in the fundamental mode and in the first overtone (cf. Table 4 in the cited paper); we also compute the Galactic rotation angular speed $\Omega(R_G)$ at the position of each Cepheid using the rotation-curve parameters determined by Bobylev and Bajkova (2014b) (cf. Eq. (9) in this paper). We determine the angular speed of the spiral pattern, Ω_P, solving the set of equations (11) by least squares:

$$\Omega_P({\rm Car–Sgr}) = 26.0 \pm 0.4 \text{ km s}^{-1} \text{ kpc}^{-1}. \qquad (12)$$

We similarly determine the angular speed of the spiral pattern from positions of Cepheids in the Perseus arm ($\alpha_{\rm maser} = +0.200$ and $\tan i_{\rm maser} = -0.207$) and in the Outer arm ($\alpha_{\rm maser} = +0.563$ and $\tan i_{\rm maser} = -0.214$) assuming that the rotation curve determined, within $R_G < 1.15R_0$, by parameters from Eq. (9) in Bobylev and Bajkova (2014b) becomes flat beyond $R_G > 1.15R_0$:

$$\Omega_P({\rm Per}) = 24.5 \pm 0.4 \text{ km s}^{-1} \text{ kpc}^{-1}, \qquad (13)$$
$$\Omega_P({\rm Outer}) = 25.0 \pm 0.5 \text{ km s}^{-1} \text{ kpc}^{-1}.$$

The three estimates agree excellently with each other, but differ strongly from that obtained from Cepheids of the Inner arm:

$$\Omega_P({\rm Inner}) = 7 \pm 3 \text{ km s}^{-1} \text{ kpc}^{-1}. \qquad (14)$$

The discrepancy is possibly due to (1) the fact that the second-order expansion fails to properly describe the rotation curve from Bobylev and Bajkova (2014b) for small galactocentric distances and (2) the wrong estimate of the Inner arm's parameters in Bobylev and Bajkova (2014a), where it is based on only three masers. Thus, our final estimate of the spiral pattern's angular speed is the mean value for the three main arms:

$$\langle\Omega_P\rangle = 25.2 \pm 0.5 \text{ km s}^{-1} \text{ kpc}^{-1}. \qquad (15)$$

This result is consistent with recent independent determinations of the angular speed of the spiral pattern, mainly between 20 and 30 km s^{-1} kpc^{-1} (Gerhard 2011), with the estimates obtained by Dias and

Lépine (2005) from computations of "birth sites" for 212 young open clusters with complete kinematical data: $\Omega_P = 24-26$ km s^{-1} kpc^{-1}, and with the recent estimate by Junqueira et al. (2015), based on their study of the correlation between the change of energy and angular momentum of open clusters induced by the spiral density wave: $\Omega_P = 23.0 \pm 0.5$ km s^{-1} kpc^{-1}.

CONCLUSIONS

Our analysis of the spatial distribution of 565 classical Cepheids within ∼5 kpc from the Sun revealed the present of four fragments of the global spiral pattern. Note that the Outer arm, the most distant one from the center, is actually identified from newly discovered Cepheids. Among them, the most clearly expressed one is the spiral fragment in the region of the Carina–Sagittarius arm, traced by a chain of 76 Cepheids along a narrow spiral with a pitch angle about 10.5° and a cross-arm rms width about 80 pc. We also found a chain of 23 Cepheids located beyond the Carina–Sagittarius arm, along a spiral fragment with practically the same pitch angle (∼10.0°) and the rms transversal width ∼100 pc. The two spiral condensations beyond the Solar circle (representing respectively the Perseus arm and the Outer arm) are much broader; their pitch angles are estimated as ∼8.0° and ∼10.9°. The rms cross-arm widths of the Perseus and Outer arms traced by Cepheids are about 600 pc. The spiral fragments we identified can be fitted to a four-armed global grand-design spiral pattern, if we adopt its pitch angle $i = 9.5° \pm 0.1°$. We also estimate the angular speed of the spiral pattern, $\langle\Omega_P\rangle$, to be 25.2 ± 0.5 km s^{-1} kpc^{-1}, in a good agreement with most of recent determinations, based on different techniques.

ACKNOWLEDGMENTS

This study was financially supported by the Russian Foundation for Basic Research (project nos. 13-02-00203 and 14-02-00472). Determinations of light-curve parameters and distances of Cepheids were supported by the Russian Scientific Foundation (project no. 14-22-00041).

REFERENCES

1. L. N. Berdnikov, Odessa Astron. Publ. **18**, 23 (2006).
2. L. N. Berdnikov, VizieR On-line Data Catalog: CDS II/285 (2008).
3. L. N. Berdnikov, A. K. Dambis, and O. V. Vozyakova, Astron. Astrophys. Suppl. Ser. **143**, 211 (2000).
4. L. N. Berdnikov, A. Yu. Kniazev, V. V. Kravtsov, E. N. Pastukhova, and D. G. Turner, Astron. Lett. **35**, 35 (2009a).
5. L. N. Berdnikov, A. Yu. Kniazev, V. V. Kravtsov, E. N. Pastukhova, and D. G. Turner, Astron. Lett. **35**, 311 (2009b).
6. L. N. Berdnikov, A. Yu. Kniazev, R. Sefako, V. V. Kravtsov, E. N. Pastukhova, and S. V. Zhuiko, Astron. Rep. **55**, 816 (2011).
7. L. N. Berdnikov, A. Yu. Kniazev, R. Sefako, V. V. Kravtsov, and S. V. Zhuiko, Astron. Lett. **40**, 125 (2014).
8. L. N. Berdnikov, A. Yu. Kniazev, R. Sefako, A. K. Dambis, V. V. Kravtsov, and S. V. Zhuiko, Astron. Lett. **41**, 23 (2015).
9. L. N. Berdnikov, O. V. Vozyakova, and A. K. Dambis, Astron. Lett. **22**, 839 (1996).
10. V. V. Bobylev and A. T. Bajkova, Astron. Lett. **39**, 759 (2013).
11. V. V. Bobylev and A. T. Bajkova, Mon. Not. R. Astron. Soc. **437**, 1549 (2014a).
12. V. V. Bobylev and A. T. Bajkova, Astron. Lett. **40**, 773 (2014b).
13. G. Bono, M. Marconi, S. Cassisi, F. Caputo, W. Gieren, and G. Pietrzynski, Astrophys. J. **621**, 966 (2005).
14. A. W. J. Cousins, Mon. Not. R. Astron. Soc. **81**, 25 (1976).
15. J. F. Dean, P. R. Warren, and A. W. J. Cousins, Mon. Not. R. Astron. Soc. **183**, 569 (1978).
16. W. S. Dias and J. Lépine, Astrophys. J. **629**, 825 (2005).
17. Yu. N. Efremov, Astron. Rep. **55**, 108 (2011).
18. P. Englmaier and O. Gerhard, Mon. Not. R. Astron. Soc. **304**, 512 (1999).
19. P. Englmaier, M. Pohl, and N. Bissantz, Mem. Soc. Astron. Ital. Suppl. **18**, 199 (2011).
20. P. Fouque, P. Arriagada, J. Storm, T. G. Barnes, N. Nardetto, A. Merand, P. Kervella, W. Gieren, D. Bersier, G. F. Benedict, and B. E. McArthur, Astron. Astrophys. **476**, 73 (2007).
21. O. Gerhard, Mem. Soc. Astron. Ital. Suppl. **18**, 185 (2011).
22. C. Guerra and V. Pascucci, IEICE Trans. Inf. Syst. **E84-D**, 1739 (2001).
23. L. G. Houl, J. L. Han, and W. B. Shi, Astron. Astrophys. **499**, 473 (2009).
24. T. C. Junqueira, C. Chiappini, J. R. D. Lépine, I. Minchev, and B. X. Santiago, Mon. Not. R. Astron. Soc. **449**, 2336 (2015).
25. S. Kendall, C. Clarke, and R. C. Kennicutt, Mon. Not. R. Astron. Soc. **446**, 4155 (2015).
26. R. C. Kennicutt and P. Hodge, Astrophys. J. **253**, 101 (1982).
27. M. K. Kim, T. Hirota, M. Honma, H. Kobayashi, T. Bushimata, Y. K. Choi, H. Imai, K. Iwadate, et al., Publ. Astron. Soc. Jpn. **60**, 991 (2008).

28. M. Kodric, A. Riffeser, U. Hopp, S. Seitz, J. Koppenhoefer, R. Bender, C. Goessl, J. Snigula, et al., Astron. J. **145**, 106 (2013).
29. E. S. Levine, L. Blitz, and C. Heiles, Science **312**, 1773 (2006).
30. H. Nakanishi and Y. Sofue, Publ. Astron. Soc. Jpn. **55**, 191 (2003).
31. M. Pohl, P. Englmaier, and N. Bissantz, Astrophys. J. **677**, 283 (2008).
32. G. Pojmanski, Acta Astron. **52**, 397 (2002).
33. M. J. Reid, K. M. Menten, X. W. Zheng, A. Brunthaler, L. Moscadelli, Y. Xu, B. Zhang, M. Sato, M. Honma, T. Hirota, K. Hachisuka, Y. K. Choi, G. A. Moellenbrock, and A. Bartkiewicz, Astrophys. J. **700**, 137 (2009).
34. D. Russeil, Astron. Astrophys. **397**, 133 (2003).
35. K. L. J. Rygl, A. Brunthaler, M. J. Reid, K. M. Menten, H. J. van Langevelde, and Y. Xu, Astron. Astrophys. **511**, 2 (2010).
36. N. N. Samus, O. V. Durlevich, E. V. Kazarovets, N. N. Kireeva, E. N. Pastukhova, A. V. Zharova, et al., VizieR On-line Data Catalog: B/gcvs (2007–2012).